The Influence of Elevation Angle on 60 GHz Near-Body Path Gain

The Influence of Elevation Angle on 60 GHz Near-Body Path Gain

Lei Zhang, Adrian McKernan, Simon L. Cotton, and William G. Scanlon
Centre for Wireless Innovation, ECIT Institute
Queen's University of Belfast, Belfast, BT3 9DT, U.K.
Email:{lzhang27, a.mckernan, simon.cotton, w.scanlon}@qub.ac.uk

***Abstract*—Indoor millimeter-wave wireless access points will necessarily be placed relatively high on walls and ceilings to reduce shadowing and blocking effects and to improve coverage. This means that the access point will be at a range of elevation angles with respect to the user equipment. A series of experiments were conducted in an anechoic chamber to investigate the influence of elevation angle on non-line-of-sight near-body path gain at 60 GHz. An analysis of the measurement results shows that, compared to low elevation angle scenarios, high elevation angles of incidence provide better performance at 60 GHz with between 10 dB and 15 dB higher path gain.**

***Index Terms*—Body shadowing, channel measurements, millimeter-wave, path gain.**

I. Introduction

The currently underutilized millimeter-wave (mm-wave) bands are being considered as a possible solution to enhance capacity in future 5G networks [1]. In the unlicensed 60 GHz band in particular, there is between 5–7 GHz of bandwidth available worldwide. Because of this spectrum availability and propagation characteristics which naturally support shorter-range systems, it is unsurprising that the 60 GHz band is being exploited to support dense small cell networks [2]. One of the obstacles which may prevent future network densification is the fact that wireless signals at these frequencies are extremely sensitive to blockage by obstacles such as the human body [3].

There have been a number of studies investigating human body effects on the 60 GHz channel. For example, in [4] a statistical body shadowing model was combined with numerical ray-determination methods. In [5], propagation characteristics, such as the signal attenuation and coherence bandwidth were used to analyze the influence of human activity on 60 GHz indoor channels through wide-band measurements. In [6], a physical optical method (Piazzi's numerical integration method) was applied by assuming that the human body can be represented as absorbing screens of infinite height. The sufficiency of this model was shown by comparison with blocking measurements at 60 GHz, which considered both single and multiple persons. In [7], the authors presented a numerical model for 60 GHz near-body channels that combined the indoor channel model standardized by IEEE 802.11ad and diffraction models by considering the human body as a circular cylinder [8]. However, all of these studies only considered azimuthal (horizontal plane) angles of incidence.

In near-body channels, the user equipment (UE) is positioned physically close to the human body during use. Everyday operation of laptops, tablets and smartphones falls into this category of use cases. It is worth highlighting that at 60 GHz these devices are operated at a significant number of wavelengths away from the user's body and are therefore in the far-field region. As a result, the overall system performance can be influenced by scattering and attenuation due to the user's body and the relative positioning and orientation of the UE. Furthermore, the effects of different antenna types at mm-wave bands should also be considered. For example, for high-gain and low-beamwidth antenna systems, the human body can dramatically degrade the signal power by significantly shadowing the main propagation paths between the transmitter and receiver [9] [10].

In dense small cell indoor mm-wave deployments there has also been increasing interest in low-gain, wide-beamwidth antenna solutions, especially as the access point (AP) to UE path lengths may be relatively short. The potential benefit arises due to the increased beamwidth at the AP antenna permitting the reception of signals arriving from a broader range of angles, including both line of sight (LOS) and multipath propagation. To make the most of the benefits brought about by low-gain and wide-beamwidth antenna systems, placing the AP at higher elevations has been considered as a possible solution to improve the channel performance for indoor small cell applications [11]. However, for such systems, an understanding of how the elevation angle of incidence affects near-body mm-wave channels has yet to be determined. As a first step to addressing this, in this paper we experimentally investigate the 60 GHz wireless non-LOS (NLOS) near-body path gain at a range of elevation angles within an anechoic chamber.

The remainder of this paper is organized as follows: Section II introduces the 60 GHz near-body channel measurement set-up and scenarios. In Section III, the measurement results and statistical analysis are described, with the conclusions presented in Section IV.

II. Measurement Set-Up and Scenario

A. Measurement Set-Up

The measurements reported in this paper were conducted in the anechoic chamber of the ECIT Institute, Queen's University, Belfast, UK. The custom 60 GHz near-body channel measurement system was based on the Hittite HMC6000LP711 transmitter (TX) and Hittite HMC6001LP711E receiver (RX)

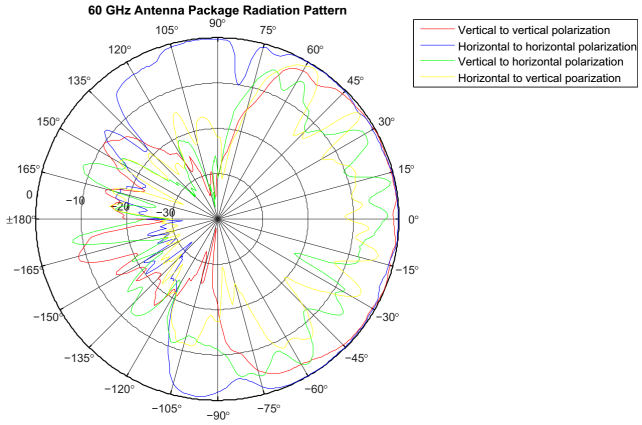

Fig. 1: Measured RX module normalized antenna gain patterns at 60 GHz.

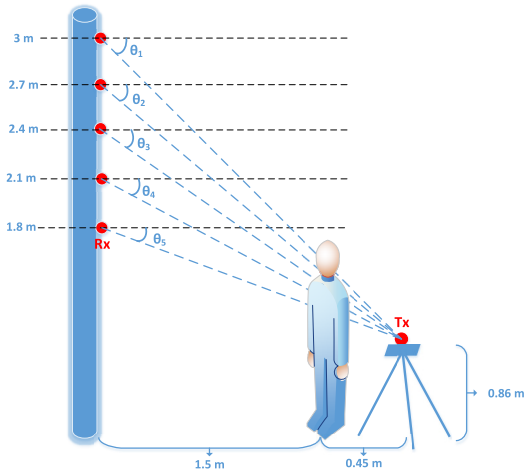

Fig. 2: Geometry of the measurement scenario.

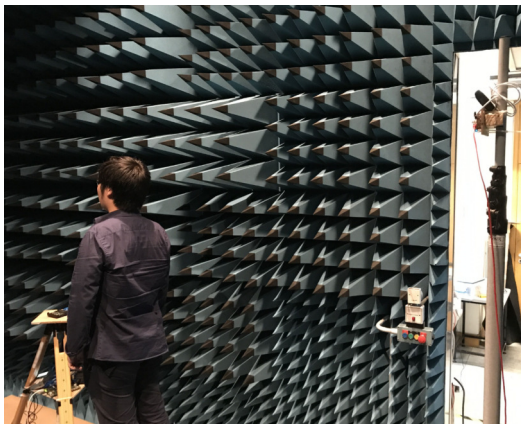

Fig. 3: 60 GHz near-body channel measurement set-up.

modules manufactured by Analog Devices. Both modules utilize an identical linearly-polarized antenna-in-package with +7.5 dBi gain. The measured normalized gain patterns of the RX module are shown in Fig. 1 [12] [13]. The measured half power beam width of the antenna-in-package is approximately 120°. The near-body UE was represented by the TX module which was mounted on a compact ABS enclosure (80 mm × 80 mm × 20 mm) and fixed at a height of 86 cm using a wooden tripod. The antenna boresight was facing upwards (towards the zenith) with horizontal polarization. The RX module was fixed to a Watson Radio (model TFM-20-2) telescopic fiber glass mast, which is height adjustable to 6.1 m. In all but one case (outlined below), the RX module was arranged to ensure that the antenna was co-polarized (horizontal polarization) with the TX module with the boresight directed towards the floor of the anechoic chamber.

B. Measurement Scenario

The geometry of the measurement scenario is shown in Fig. 2. For the with-body measurements, the test user, an adult male of height of 1.72 m and mass 75 kg, stood upright, centred at a distance of 1.5 m to the fiber glass mast. The UE (TX) tripod was placed on the other side of the user's body at a distance of 45 cm from the body center-line. To investigate the effects of various elevation angles of incidence ($\theta_1 = 47.6°$ to $\theta_5 = 25.7°$), the RX module was placed at 5 discrete heights from 3 m to 1.8 m in 30 cm intervals.

At the beginning of each measurement, the TX was configured to transmit a continuous wave signal at 60.05 GHz with an Equivalent Isotropically Radiated Power (EIRP) of +10.9 dBm. The received power was then recorded without the test user present to provide a reference case. This allowed the elimination of factors such as the slightly different path lengths due to the angular geometry and equipment positioning inaccuracies. The measurement was then repeated with the test user present. Since the test user cannot stand perfectly still, the 'with-body' measurement was repeated to allow consideration of unintended movement effects. The received signal power was recorded using a v1.4 Red Pitaya data acquisition platform at a sample rate of 96 kHz. The duration of each measurement was set to 20 s (1,920,000 samples). Fig. 3 shows the measurement set-up with the test user present with the tripod to the left of the user and the RX mast at the right of the figure. It should be noted that the test user always faced the UE (TX) and the TX and RX modules were co-polarised (horizontal polarization) for all 5 heights. Additionally, since the 1.8 m height case is very close to the test user's height (meaning that the boresight of TX and RX antennas would be facing in opposite directions), an extra measurement case was introduced for this height with the TX and RX modules re-oriented so that their boresights were directed towards the test user with vertical polarization.

[1]https://redpitaya.com/ (visited on 10/21/2017)

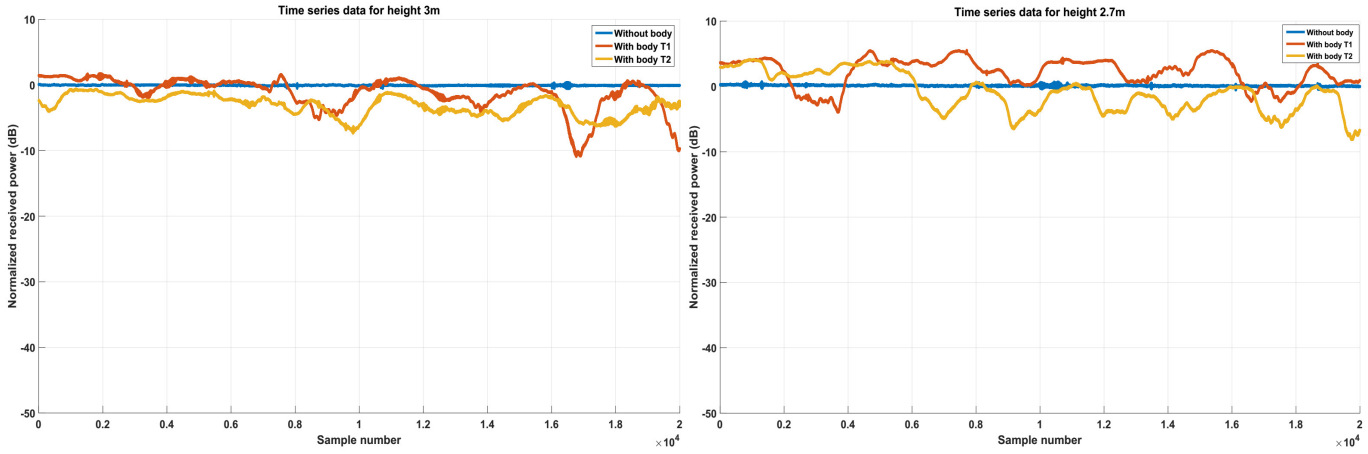

(a) Time series data for height 3m.

(b) Time series data for height 2.7m.

Fig. 4: Time series data for height 3m and 2.7m.

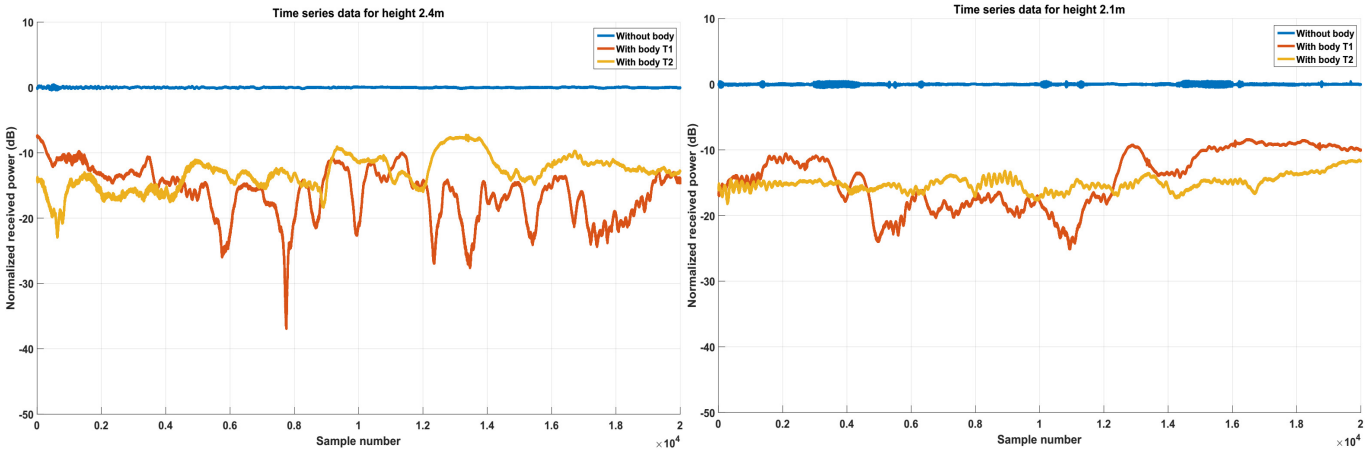

(a) Time series data for height 2.4m.

(b) Time series data for height 2.1m.

Fig. 5: Time series data for height 2.4m and 2.1m.

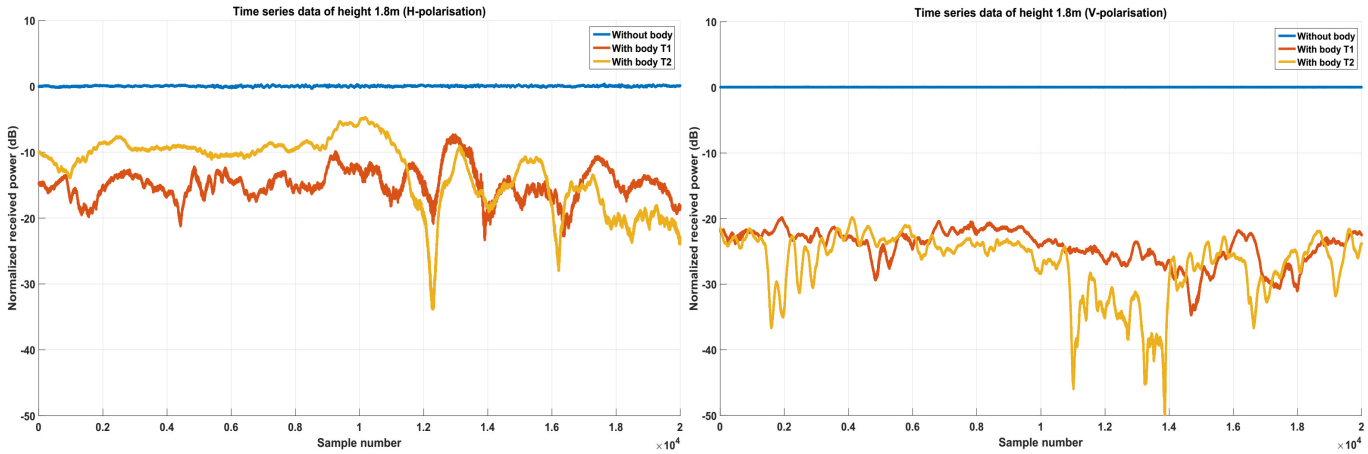

(a) Time series data for height 1.8m (horizontal polarization).

(b) Time series data for height 1.8m (vertical polarization).

Fig. 6: Time series data for height 1.8m (horizontal and vertical polarization).

Height	Body Shadowing Factor (dB) $(\mu - \mu_0)$	Increase in the Standard Deviation (dB) $(\sigma - \sigma_0)$
3 m, trial 1	-1.2 dB	$+2.4$ dB
3 m, trial 2	-3.1 dB	$+1.4$ dB
2.7 m, trial 1	$+2.0$ dB	$+2.0$ dB
2.7 m, trial 2	-1.0 dB	$+2.8$ dB
2.4 m, trial 1	-16.0 dB	$+3.8$ dB
2.4 m, trial 2	-13.0 dB	$+2.4$ dB
2.1 m, trial 1	-14.4 dB	$+4.2$ dB
2.1 m, trial 2	-15.0 dB	$+1.1$ dB
1.8 m, trial 1	-14.7 dB	$+2.2$ dB
1.8 m, trial 2	-13.5 dB	$+4.7$ dB
1.8 m, trial 1 (V-polarization)	-24.3 dB	$+2.6$ dB
1.8 m, trial 2 (V-polarization)	-26.8 dB	$+4.7$ dB

TABLE I: Summary of results.

III. Results and Analysis

An averaging window of fixed size n $(n = 96)$ was applied to the measurement data to improve the signal to noise ratio performance. This downsampled the raw received signal power to $1,920,000/96 = 20,000$ time series points, giving an effective sampling rate of 1 kHz. Following this, the time series data was normalized to the mean value of the received signal power of the reference measurement (i.e., 'without-body') for each measurement height. The normalized received signal power time series data for RX heights of 3 m to 1.8 m are presented in Fig. 4 to Fig. 6. A visual inspection of the 'with-body' and 'without-body' results shows that the presence of the user has a significant effect on the 60 GHz near-body channel. It is also evident that there can be significant link attenuation and, despite the care taken to minimize the motion artefacts in these stationary measurements, even small movements seem to have had a considerable impact on the observed channel.

Firstly, considering the 'without-body' case (in particular the samples in the range from 0.3×10^4 to 0.45×10^4 and 1.4×10^4 to 1.6×10^4) depicted in Fig. 5b. Since the measurements were undertaken for a static scenario, the observed variations were caused by a combination of measurement system noise and, given the short wavelength, equipment vibrations. Likewise, for the 'with-body' cases, the uncertainty of the user positioning and any unintended movements also need to be considered. Therefore, to investigate any perturbations in the path gain brought about the presence of the user, the mean (denoted as μ and μ_0 for 'with-body' and 'without-body' cases, respectively) and standard deviation (σ and σ_0) values of the logarithmic transformed received signal power were calculated. The body shadowing factor $(\mu - \mu_0)$ and the increase in the standard deviation $(\sigma - \sigma_0)$ when moving from the 'without-body' to the 'with-body' cases are summarized in Table I.

The benefits of utilizing high elevation angles for near-body to AP channels, e.g., for RX heights of 3 m and 2.7 m, can be clearly seen in the Table I, where the body shadowing factor is between $+2.0$ dB and -3.1 dB compared to values of -20 dB to -40 dB reported for azimuthal (horizontal plane) incidence in elsewhere [6] [10]. Also, higher elevations show less received signal power variation for the stationary user: e.g., the increase in the standard deviation for the RX heights of 2.4 m and 2.1 m is much higher than for the 3 m and 2.7 m cases. This is mainly because the geometry is such that the direct path may only be partially shadowed (if at all) by the user's head in the higher elevation cases. Indeed, there was a positive body shadowing factor for one of the trials at 2.7 m height (Fig. 4b) which suggests that there was a significant component reflected off the test-user's body providing signal enhancement. Furthermore, the wide-beamwidth antennas used in the measurement system have the ability to capture significantly more scattered wave energy under NLOS scenarios, which corresponds to the conclusion in [14]. This effect can be further verified by inspecting the results for the lower elevations, e.g., for the RX heights of 2.1 m and 2.4 m the shadowing factor increases to between -13.0 dB and -16.0 dB.

The effect of polarization under low elevation circumstances can be seen by comparing the horizontal and vertical polarization results at the height of 1.8 m. Compared to the horizontal polarization case, the body shadowing factor for vertical polarization increases from between -13.5 dB and -14.7 dB to between -24.3 dB and -26.8 dB. These increased body shadowing factors are now closer to the azimuthal incidence cases already reported in the literature. However, the degree to which wave polarization is the cause of the increased shadowing cannot be determined from these results since the TX and RX antenna boresight directions are now directly towards the user rather than towards the ceiling and the floor of the anechoic chamber, respectively.

IV. Conclusion

In this work, we have experimentally investigated the influence of elevation angle of incidence on 60 GHz near-body path gain using low-gain, wide-beamwidth antennas. The scenarios considered included various elevation angles, with and without a test-user present and different polarizations for the lowest elevation case. The results show that the near-body path gain can be dramatically improved by as much as 10 dB to 15 dB by increasing the elevation angle of incidence for near-body UEs. This is achieved by ensuring that the mm-

wave access points are placed at relatively high heights and at close spacing. Furthermore, under low angle of elevation circumstances, horizontal polarization outperforms vertical polarization by up to 13 dB. Due to the short wavelength involved, channel variations were observed in time series data for stationary measurements even without the user present, most likely associated with equipment vibrations. For the 'with-body' measurements, user positioning uncertainties and unintended movements were found to be more significant at this frequency. Therefore, there is a need for improved experimental techniques and methodologies for future studies of user effects on 60 GHz channels.

ACKNOWLEDGMENT

The work was funded in part by the Northern Ireland Department for the Economy as part of the US-Ireland NEMOs project reference USI 080.

REFERENCES

[1] T. S. Rappaport, S. Sun, R. Mayzus, H. Zhao, Y. Azar, K. Wang, G. N. Wong, J. K. Schulz, M. Samimi, and F. Gutierrez, "Millimeter wave mobile communications for 5G cellular: It will work!" *IEEE Access*, vol. 1, pp. 335–349, 2013.

[2] P. Smulders, "Exploiting the 60 GHz band for local wireless multimedia access: Prospects and future directions," *IEEE Communications Magazine*, vol. 40, no. 1, pp. 140–147, 2002.

[3] Y. Niu, Y. Li, D. Jin, L. Su, and A. V. Vasilakos, "A survey of millimeter wave communications (mmwave) for 5G: opportunities and challenges," *Wireless Networks*, vol. 21, no. 8, pp. 2657–2676, 2015.

[4] S. Obayashi and J. Zander, "A body-shadowing model for indoor radio communication environments," *IEEE Transactions on Antennas and Propagation*, vol. 46, no. 6, pp. 920–927, 1998.

[5] S. Collonge, G. Zaharia, and G. E. Zein, "Influence of the human activity on wide-band characteristics of the 60 GHz indoor radio channel," *IEEE Transactions on Wireless Communications*, vol. 3, no. 6, pp. 2396–2406, 2004.

[6] J. S. Lu, D. Steinbach, P. Cabrol, and P. Pietraski, "Modeling human blockers in millimeter wave radio links," *ZTE Communications*, vol. 10, no. 4, pp. 23–28, 2012.

[7] T. Mavridis, L. Petrillo, J. Sarrazin, A. Benlarbi-Delai, and P. De Doncker, "Near-body shadowing analysis at 60 GHz," *IEEE Transactions on Antennas and Propagation*, vol. 63, no. 10, pp. 4505–4511, 2015.

[8] T. Mavridis, L. Petrillo, J. Sarrazin, D. Lautru, A. Benlarbi-Delai, and P. De Doncker, "Creeping wave model of diffraction of an obliquely incident plane wave by a circular cylinder at 60 GHz," *IEEE Transactions on Antennas and propagation*, vol. 62, no. 3, pp. 1372–1377, 2014.

[9] C. Gustafson and F. Tufvesson, "Characterization of 60 GHz shadowing by human bodies and simple phantoms," in *6th European Conf. on Antennas and Propagation (EUCAP)*, 2012, pp. 473–477.

[10] M. Fakharzadeh, J. Ahmadi-Shokouh, B. Biglarbegian, M. Nezhad-Ahmadi, and S. Safavi-Naeini, "The effect of human body on indoor radio wave propagation at 57–64 GHz," in *IEEE Intl. Symp. on Antennas and Propagation (APSURSI)*, 2009, pp. 1–4.

[11] S. K. Yoo, S. L. Cotton, R. W. Heath, and Y. J. Chun, "Measurements of the 60 GHz UE to eNB channel for small cell deployments," *IEEE Wireless Communications Letters*, vol. 6, no. 2, pp. 178–181, 2017.

[12] "Analog Device HMC6000LP711E: Millimeterwave Transmitter 57-64 GHz Data Sheet," Link: http://www.analog.com/media/en/technical-documentation/data-sheets/hmc6000.pdf, accessed: 2017-10-28.

[13] "Analog Device HMC6001LP711E: Millimeterwave Receiver 57-64 GHz Data Sheet," Link: http://www.analog.com/media/en/technical-documentation/data-sheets/hmc6001.pdf, accessed: 2017-10-28.

[14] S. Rajagopal, S. Abu-Surra, and M. Malmirchegini, "Channel feasibility for outdoor non-line-of-sight mmwave mobile communication," in *IEEE Vehicular Technology Conference (VTC Fall)*, 2012, pp. 1–6.